NANOSECOND DECAY STUDIES OF A FLUORESCENCE PROBE BOUND TO APOMYOGLOBIN

ARI GAFNI, ROBERT P. DETOMA, RICHARD E. MANROW, *and* LUDWIG BRAND,
Biology Department and McCollum-Pratt Institute,
The Johns Hopkins University,
Baltimore, Maryland 21218

ABSTRACT Excited state interactions of *N*-(*p*-tolyl)-2-aminonaphthalene-6-sulfonate (2,6 *p*-TNS) bound to apomyoglobin were studied by nanosecond time-resolved emission spectroscopy. A dynamic interaction of the excited dye molecule with its binding site, associated with a significant change in the emission energy with time, was observed. The decay kinetics were found to be complex and consistent with the kinetic model for solvent relaxation as proposed by Bakhshiev et al. (*Opt. Spectrosc.* **21**:307. 1966.). The behavior of 2,6 *p*-TNS bound to apomyoglobin was found to be qualitatively similar to that of the dye dissolved in a viscous solvent such as glycerol or adsorbed to egg lecithin vesicles. The detailed information obtained by following the changes in emission spectra of fluorescent probes on the nanosecond time scale leads to a better understanding of their interactions with biological systems.

INTRODUCTION

Weber and Laurence (1954) reported that 1-anilinonaphthalene-8-sulfonate (1,8 ANS)[1] showed intense blue fluorescence when adsorbed to serum albumin in contrast to a very weak green emission found in aqueous solution. The subsequent studies by Stryer (1965) suggesting that this dye adsorbed to the heme binding site of apomyoglobin and the findings that the dye adsorbed to chymotrypsin and chymotrypsinogen (McClure and Edelman, 1966) and to alcohol dehydrogenase (Brand et al., 1967) stimulated further interest in the use of *N*-arylaminonaphthalene dyes as fluorescence probes (Edelman and McClure, 1968). These dyes have been shown to interact with a variety of materials of biochemical interest, including proteins and membranes (see Brand and Gohlke, 1972, for a review). For this reason there has been considerable interest in understanding how solvent environment affects their fluorescence.

It appears that in spite of the extensive work already reported on the spectroscopy and photophysics of *N*-arylaminonaphthalenes, many aspects of their excited-state behavior, even in simple solvents, still remain to be resolved. Some of these are based on the potential ability of the excited probe to undergo (*a*) a direct dipole moment

[1] *Abbreviations used in this paper:* 1,8 ANS, 1-anilinonaphthalene 8-sulfonate); 2,6 *p*-TNS, *N*-(*p*-tolyl)-2-aminonaphthalene-6-sulfonate.

change during vibrational relaxation (Stryer, 1965; Seliskar and Brand, 1971; Smith and Woody, 1976), (*b*) specific photoassociation with polar solvent molecules (Greene, 1975; DeToma et al., 1976), (*c*) molecular relaxation subsequent to Franck-Condon excitation (Weber and Laurence, 1954; Penzer, 1972; Kosower et al., 1975), and (*d*) spectroscopic state inversion or mixing (Li et al., 1975). The consequences of these processes are to prepare unitary, dual, or multiple excited-state systems in which at least one of the components is highly polar. Quite often the fundamental *process* of solvent interaction which leads to or follows state preparation is ignored and vague terms such as "solvent-stabilized", "solvent-sensitive" or "solvent-induced" are commonly employed. The tacit meaning of these terms in many cases is very clearly dipolar orientational relaxation of polar solvent molecules around the prepared excited state(s) of the solute (solvent relaxation). The importance of this fundamental process when dealing with highly polar excited states and its dynamic influence on the fluorescence of probes in polar environments of restricted mobility cannot be ignored.

In spite of the potentially complicated photophysical behavior of the *N*-arylaminonaphthalene dyes, questions of interest can be raised regarding the excited-state interactions of these fluorophores when bound to proteins. The work reported here describes the emission-wavelength dependence and the temperature dependence of the fluorescence decay kinetics of *N*-(*p*-tolyl)-2-aminonaphthalene-6-sulfonate (2, 6 *p*-TNS) adsorbed to apomyoglobin. This system is particularly interesting since Stryer (1965) and Anderson et al. (1970) indicated that 1, 8 ANS binds to this protein at the region where heme is normally bound. The time-resolved spectral properties presented are essentially free from the convolution artifact. To our knowledge this is the first report where *deconvolved* time-resolved emission spectra have been obtained for a protein-dye complex. The experiments to be described address the following questions. Does the steady-state emission spectrum depend on excited-state interactions taking place on the nanosecond time scale? Does the 2, 6 *p*-TNS excited-state interaction with the binding site environment on apomyoglobin resemble a continuous dipolar relaxation process? More specifically, are there any significant nanosecond motions of polar residues at the 2,6 *p*-TNS binding site? How does the decay behavior of 2,6 *p*-TNS adsorbed to apomyoglobin compare to that observed with the dye dissolved in glycerol or adsorbed to liposomes (DeToma et al., 1976)?

METHODS

Materials

Sperm whale sketetal muscle myoglobin was obtained from Sigma Chemical Co., St. Louis, Mo. 2,6 *p*-TNS was prepared by Carl Seliskar (Seliskar and Brand, 1971). A stock solution was prepared in 0.1 M phosphate buffer, pH 6.8. Any undissolved dye was removed by Millipore filtration (GS, 0.22 μm, Millipore Corp., Bedford, Mass.). The concentration of 2,6 *p*-TNS was determined spectrophotometrically with an extinction coefficient of 6.64×10^3 at 350 nm. Bovine hemin was obtained from Sigma Chemical Co. It was dissolved in 0.1 N NaOH and then diluted into distilled water to make stock solutions of about 20 mM. The concentration of hemin was determined spectrophotometrically as the pyridine-hemachromagen by assuming an

extinction of 1.0 at 557 nm for a 28.8 μM solution. Apomyoglobin was prepared according to the procedure of Theorell and Åkeson (1955). 200 mg of myoglobin were dissolved in 20 ml deionized water and dialyzed against deionized water for 48 h with several changes. The heme was removed by adding the dialyzed myoglobin solution dropwise into a swirling solution of 400 ml reagent grade acetone and 0.8 ml 1 N HCl at -14 to -16°C. Most of the resulting supernatant was drawn off, and the precipitated apomyoglobin was pelleted by centrifugation at 6,000 *g* for 10 min at -14°C. The pellets were resuspended in a small volume of bicarbonate buffer (50 mg sodium bicarbonate in 1 liter deionized water), and the apoprotein was dialyzed for 24 h against 1 liter of the same buffer. This was followed by dialysis for 48 h against 1 liter of 0.1 M phosphate buffer, pH 6.8, with one change of the buffer after 24 h. The apoprotein was stored in the cold and dark and remained stable for about 3 wk. The concentration of apomyoglobin was determined spectrophotometrically with an extinction coefficient of 1.58×10^4 at 280 nm in 0.1 M phosphate, pH 6.8 (Stryer, 1965). Fluorescence decay measurements and the analysis of data (nonlinear least squares), including the generation of nanosecond time-resolved emission spectra, were carried out as described by Easter et al. (1976). The concentration of apomyoglobin was $\sim 4 \times 10^{-5}$ M and the concentration of 2,6 *p*-TNS was $\sim 10^{-5}$ M. Excitation with an air-flash lamp through a Baird Atomic 3,300 Å filter (Baird Atomic, Inc., Bedford, Mass.) gave an effective excitation wavelength near 336 nm. To avoid interfering effects due to decay of emission anisotropy (Shinitzky, 1972), the exciting light was transmitted through a depolarizing quartz wedge and the emission was observed through a Polacoat polarizer (Raven Screen Corp., New York) whose axis was at 55°44′ to the excitation observation plane. The data for a set of time-resolved emission spectra took 3–4 days to obtain. In the experiments done at 4°C, one sample was used during the entire collection period. For the 20°C data, the cuvette solution was changed every 12 h. A stock sample was maintained in the cold and the dark. Control experiments demonstrated that samples were stable at 20°C for more than 12 h.

Steady-state fluorescence spectra were obtained with the monophoton counting decay instrument in a steady-state mode. Steady-state spectra were obtained at the start and end of each series of decay measurements and there was no evidence for any photodecomposition under the low light intensity used for excitation.

RESULTS

The steady-state fluorescence emission maximum of 2,6 *p*-TNS adsorbed to apomyoglobin at 20°C is 22.9 kK and may be compared to the maxima at 20 kK in water and 23.4 kK in ethanol (Turner and Brand, 1968). These workers also reported the emission maxima of 2,6 *p*-TNS adsorbed to several proteins. The emission maxima ranged from ~ 22 kK for horse liver alcohol dehydrogenase to 22.8 kK for alkaline phosphatase. The emission maximum found with 2,6 *p*-TNS bound to apomyoglobin is thus shifted greatly toward the blue.[2]

Fluorescence titrations indicated that 2,6 *p*-TNS binds to apomyoglobin with a stoichiometry close to 1:1 and an association constant of $\sim 2.3 \times 10^5$. Addition of hemin to a mixture of 2,6 *p*-TNS and apomyoglobin resulted in loss of fluorescence.[2]

Decay curves at various emission wavelengths were obtained together with corresponding lamp profiles by the semi-simultaneous mode of data collection as previously described (Easter et al., 1976). The photomultiplier shift factor (Gafni et al., 1975) at

[2]Similar observations were reported for 1,8 ANS bound to apomyoglobin by Stryer (1965).

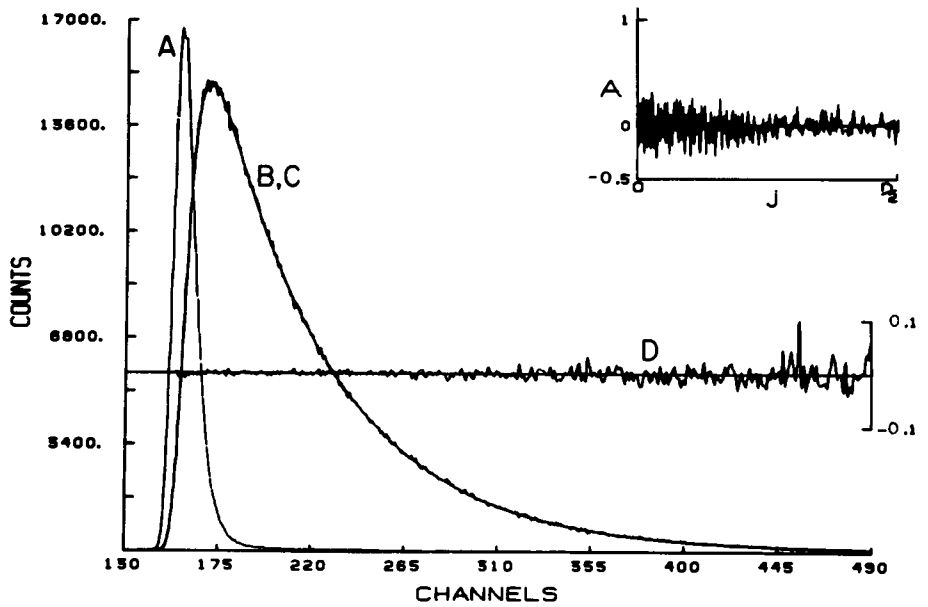

FIGURE 1 An analysis of a decay curve at 500 nm of a 2,6 *p*-TNS apomyoglobin complex at 4°C. A shows the lamp flash profile (scaled down by 20%). B shows the experimental decay curve. C shows the calculated impulse response convolved with the experimental lamp flash. D are the weighted, normalized residuals. The insert at the upper right shows the autocorrelation function of the residuals. The timing calibration was 0.204 ns/channel. 4-mm slits were used on the entrance and exit of the emission monochromator, giving a 13-nm band pass. An optical wedge and polarizer were used as described in the text to eliminate errors due to time-dependent changes in emission anisotropy.

each wavelength was determined independently with anthracene or 9-cyanoanthracene as single lifetime standards. The decay curves obtained with the apomyoglobin complex were analyzed by the method of nonlinear least squares (Easter et al., 1976). A typical result of such an analysis is shown in Fig. 1. A linear representation of the decay at 500 nm (4°C) is shown (curve B) together with the lamp flash (curve A). The theoretical decay curve based on the parameters obtained from the analysis has been convolved with the lamp flash and superimposed on the experimental curve (curve C). The visual agreement between the two curves, the randomness of the residuals (curve D) and of the autocorrelation of the residuals (upper right), together with a χ^2 value of 1.25 all indicate that the decay parameters obtained are consistent with the experimental decay data. This procedure for describing the analysis of fluorescence decay data has been discussed in more detail elsewhere (Grinvald and Steinberg, 1974; Gafni et al., 1975; Easter et al., 1976). The decay data obtained at other wavelengths were analyzed and evaluated in a similar way. This method of analysis is considered to be an empirical procedure for deconvolution. While the fluorescence decay at each wavelength was analyzed in terms of sums and differences of exponential terms, this in no way proves that the fluorescence decay is multi-exponential in character.

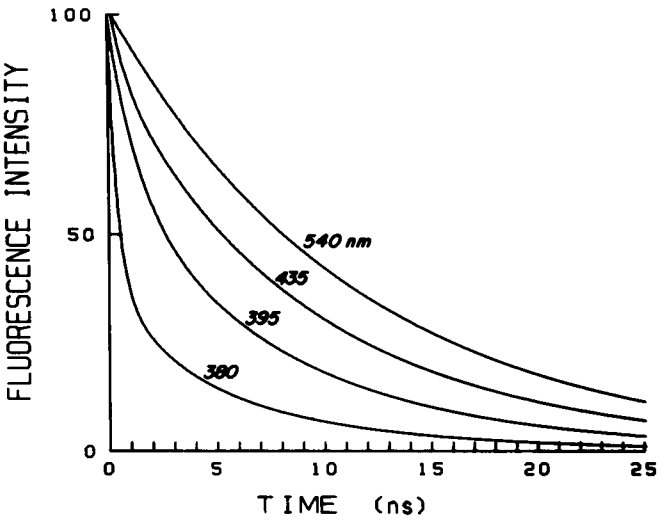

FIGURE 2 Normalized impulse response functions for a 2,6 *p*-TNS apomyoglobin complex at 4°C. Results are shown at 540, 435, 395, and 380 nm emission wavelengths. Conditions are as in Fig. 1.

Impulse response functions (deconvolved decay curves) generated from the decay parameters are shown in Fig. 2 for data obtained at emission wavelengths of 380, 395, 435, and 540 nm. It is clear that the mean decay time increases with increasing wavelength.

The variation of fluorescence decay times with emission wavelength is shown in Table I. In analyzing these data, systematic errors known to exist in our instrument, namely background, scattered light, energy-dependent timing variations in the detector, and polarization errors, were taken into account. It is clear that the decay times associated with a negative amplitude are small and with the 4°C data fall within the error estimated for the shift factor. This point will be discussed in more detail later.

Deconvolved nanosecond time-resolved emission spectra were generated from the decay data (obtained at 5-nm intervals) according to a procedure described previously (Easter et al., 1976). Three representative spectra (for 1, 9, and 50 ns) are shown in Fig. 3. These spectra are normalized for convenience of presentation. There is a clear shift of the fluorescence emission maxima to lower energies with time. Fig. 4 shows a plot of the emission maxima of the time-resolved emission spectra versus time (spectral kinetics). Curve A represents data obtained at 4°C and curve B shows the results obtained at 20°C. There is a small but significant increase in the rate of the time-dependent red shift with increased temperature. Both the rate and extent of the shift are less than observed with 2,6 *p*-TNS dissolved in glycerol. This is illustrated by the insert of Fig. 4, which compares the kinetics of the maximum shift in glycerol, curve D, to that found with the apomyoglobin complex at 4°C, curve C. It is also evident that while the complete wavelength shift can be observed in the available time window for the dye in glycerol, this is not the case for the apomyoglobin complex, where the kinetics of the wavelength shift are slow compared to the fluorescence decay.

TABLE I

EMPIRICAL DECAY PARAMETERS RECOVERED FROM THE ANALYSIS OF DECAY CURVES OBTAINED WITH A 2,6 *p*-TNS APOMYOGLOBIN COMPLEX AT 4°C and 20°C AT VARIOUS EMISSION WAVELENGTHS

At each wavelength the sum of the absolute values of the pre-exponential terms (α) was normalized to 100.

Temperature	Wavelength	α_1	τ_1	α_2	τ_2	α_3	τ_3	α_4	τ_4
°C	*nm*		*ns*		*ns*		*ns*		*ns*
20	380	58.3	0.18	22.0	2.1	19.5	7.4	0.2	13.8
	400	31.4	1.7	34.3	6.0	34.3	10.8	—	—
	420	19.0	1.9	−21.4	0.01	45.3	8.2	14.3	13.3
	440	16.7	3.2	− 6.7	0.04	56.6	8.9	20.0	12.9
	460	12.8	1.8	−15.4	0.81	48.7	8.6	23.1	12.8
	485	13.1	2.3	−18.4	0.89	65.8	10.0	2.7	19.0
	500	—	—	−37.8	0.03	22.2	7.6	40.0	11.6
	520	—	—	−18.8	0.27	53.1	9.1	28.1	13.0
	530	—	—	−14.3	0.35	53.6	9.1	32.1	12.7
	540	—	—	−16.7	5.4	50.0	7.9	33.3	12.6
4	380	59.5	0.4	19.0	2.6	17.7	7.3	3.8	12.5
	400	23.3	0.72	23.3	3.3	37.2	8.4	16.3	12.0
	420	15.7	0.66	−32.9	0.02	18.6	5.6	32.8	11.0
	440	7.9	0.94	—	—	23.7	5.4	68.4	11.1
	460	9.3	0.53	−40.0	0.01	14.7	7.0	36.0	11.6
	485	11.1	0.44	−47.6	0.03	15.9	8.7	25.4	12.3
	500	3.1	0.55	−42.2	0.004	50.0	10.6	4.7	16.3
	520	8.1	0.27	−41.9	0.04	46.8	10.9	3.2	16.4
	530	—	—	—	—	96.7	11.1	3.3	19.1
	540	—	—	−10.7	0.02	85.7	11.3	3.6	19.2

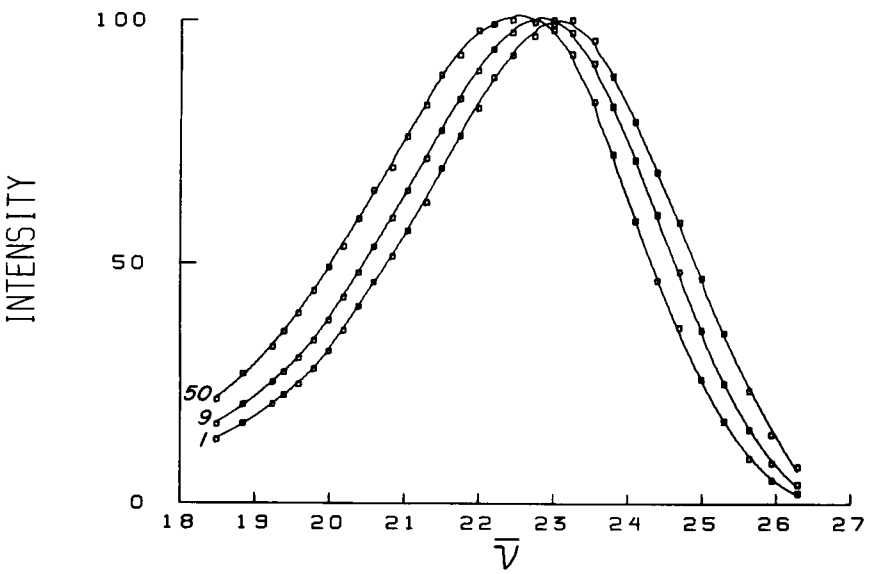

FIGURE 3 Peak normalized time-resolved emission spectra at 1, 9, and 50 ns of a 2,6 *p*-TNS apomyoglobin complex at 4°C. Conditions as in the legend to Fig. 1.

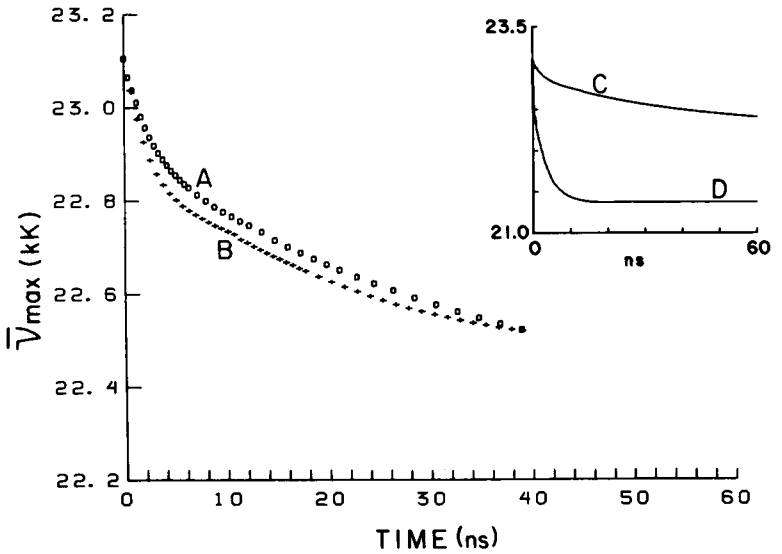

FIGURE 4 Change in the time-resolved fluorescence emission maximum with time ($\bar{\nu}_{max}(t)$) of a 2,6 *p*-TNS apomyoglobin complex and 2,6 *p*-TNS dissolved in glycerol. A (□) is 2,6 *p*-TNS apomyoglobin at 4°C. B (+) is 2,6 *p*-TNS apomyoglobin at 20°C. The insert shows C, 2,6 *p*-TNS apomyoglobin at 4°C as compared to D, 2,6 *p*-TNS in glycerol at 10°C.

The fluorescence intensity as a function of energy and time $f(\bar{\nu}, t)$, may be separated into an electronic damping term, $i(t)$, and a spectral (−intensity) shift term, $\rho(\bar{\nu}, t)$.

$$f(\bar{\nu}, t) = i(t)\,\rho(\bar{\nu}, t) \tag{1}$$

Eq. 1 is based on a model for solvent (environmental) relaxation (Bakhshiev et al., 1966; DeToma et al., 1976), where the excited solute-solvent interactions are considered to be of a universal dipolar nature. This separation of the electronic and spectral relaxation components in $f(\bar{\nu}, t)$ renders considerable simplification to the photokinetics of an excited molecular system undergoing a continuous interaction process. Plots of $\rho(\bar{\nu}, t)$ at four representative wavelengths, 380, 395, 435, and 540 nm, are shown in Fig. 5. The damping term, $i(t)$, could be recovered as a sum of two exponentials. The two decay constants and the ratio of the pre-exponential terms were the same at 4° and 20°C and are respectively: 10.2 ns, 2.1 ns, and 0.2. A nonmonoexponential representation for $i(t)$ was also observed for 2,6 *p*-TNS dissolved in glycerol and adsorbed to liposomes (DeToma et al., 1976).

DISCUSSION

The interaction of 2,6 *p*-TNS with apomyoglobin is similar to the binding of 1,8 ANS to the same protein described by Stryer (1965). The dye appears to bind at the heme binding region and the blue-shifted fluorescence emission maximum is similar to that observed when 2,6 *p*-TNS is dissolved in nonpolar solvents.

The fluorescence decay of the protein-dye complex does not show single-exponential

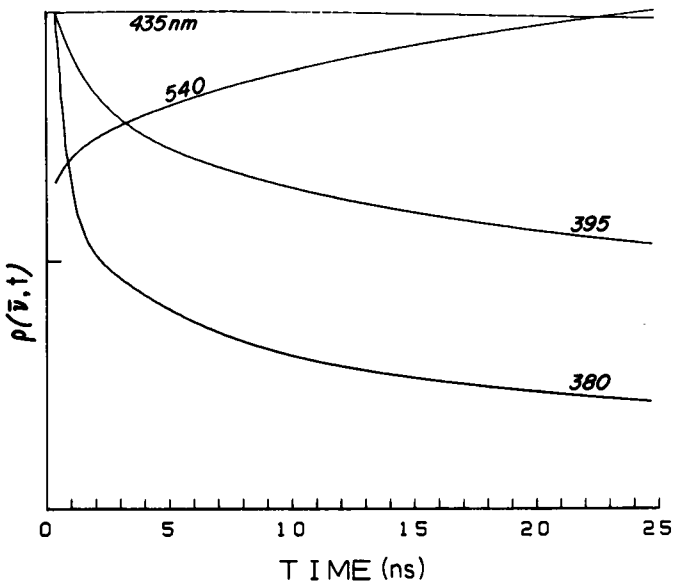

FIGURE 5 The emission energy shift functions, $\rho(\bar{\nu}, t)$, (DeToma et al., 1976) plotted against time and shown at four wavelengths. These functions are presented normalized at their maximum values in this time domain. The data is for a 2,6 *p*-TNS apomyoglobin complex at 4°C. Conditions were as for Fig. 1.

decay behavior and the mean decay time increases with increasing wavelength. The generation of deconvolved nanosecond time-resolved emission spectra reveals a significant red-shift of the emission maxima with time. These results are qualitatively similar to those obtained with 2,6 *p*-TNS dissolved in glycerol or adsorbed to liposomes (Easter et al., 1976; DeToma et al., 1976). The most likely interpretation of the decay data is that excited-state reactions are taking place. Other explanations for the wavelength dependence of the decay and the time-dependent red-shifts may also be considered.

While the 1:1 binding ratio obtained by fluorescence titration and the decrease in fluorescence upon addition of hemin suggest a unique site of interaction, binding of the dye to different conformers of apomyoglobin cannot be excluded. It is thus possible that emission from different ground-state species could in part account for the observed decay behavior. If only two ground-state species contributed to the emission, two decay times invariant with wavelength (but with wavelength-dependent preexponential terms) would be expected. This is not what has been observed. In addition it is well established that the fluorescence intensity of 2,6 *p*-TNS decreases in microenvironments where the emission maximum is shifted to the red (Brand and Gohlke, 1972; McClure and Edelman, 1968). Since it has been shown here that the mean decay time *increases* at longer wavelengths, it is unlikely that the results can be solely explained by emission from two ground-state species, one with emission to the blue of the other.

It is more reasonable to attribute the observed results to an excited-state interaction. With reference to time-dependent behavior, the most definitive evidence for excited-state reactions is the observation of a rise in the fluorescence impulse response indicating the buildup of one or more species created during the observation time window. In terms of a multiexponential impulse model, such behavior will be exposed as an exponential term(s) with a negative amplitude. The exponential component with a negative amplitude found here at the red edge with the apomyoglobin complex at 20°C is small but significant. The corresponding component in the data obtained at 4°C is so small that it falls outside the resolving power of the nanosecond decay fluorimeter.

While the presence of a negative amplitude provides *direct* evidence for an excited-state reaction, the converse is not true, i.e. its absence does not rule out an excited-state reaction on the nanosecond time-scale. If the nanosecond time-dependent spectral shifts reported here are due to excited-state environmental interactions similar in type to those described by Bakhshiev et al. (1966), there would be strong spectral overlap between the continuum of emitting species over a narrow range of spectral change ($\sim$0.6 kK). In this situation the appearance of a significant rise in the fluorescence impulse response observed at an optimal emission wavelength (low energy) depends critically on the relative rates of spectral and electronic relaxation. With a small total spectral shift and a moderately slow rate of spectral shift relative to electronic damping, a negative amplitude term in a decay curve could be easily masked even if it could be measured at an impractically long emission wavelength (low fluorescence intensity).

To illustrate this point more clearly, we consider Eq. 1 in more detail. In Eq. 1 the quantity $\rho(\bar{\nu}, t)$ introduces the spectral relaxation kinetics

$$\rho(\bar{\nu}, t) \equiv \rho(\bar{\nu} - \xi(t)), \tag{2}$$

which may be described by a position parameter $\xi(t)$ in energy units such as elementary emission maxima [$\equiv \bar{\nu}_{max}(t)$], cf. Fig. 4. At fixed t, $\rho(\bar{\nu}, t)$ represents an elementary spectral contour shifted in energy by the amount $\xi(t)$. At fixed $\bar{\nu}$, $\rho(\bar{\nu}, t)$ describes the influence of $\xi(t)$ on the fluorescence decay $f(\bar{\nu}, t)$ at that emission wavenumber.

A necessary requirement for an observable rise in $f(\bar{\nu}, t)$ is that

$$\frac{\partial f(\bar{\nu}, t)}{\partial t} > 0, \tag{3}$$

at least over the early time period in the decay of $i(t)$. Eqs. 1 and 3 further imply the following important relation between the logarithmic derivatives of $\rho(\bar{\nu}, t)$ and $i(t)$

$$\frac{\partial \ln \rho(\bar{\nu}, t)}{\partial t} > -\frac{\partial \ln i(t)}{\partial t}, \tag{4}$$

which states that the relative rate of spectral relaxation influence [$\xi(t)$ implicit in $\rho(\bar{\nu}, t)$] must be greater than the relative rate of electronic relaxation in order for there to be an observable rise in $f(\bar{\nu}, t)$. Since $\partial i(t)/\partial t] < 0$ for most systems of in-

terest and $i(t)$, $\rho(\bar{\nu}, t) > 0$, it follows that

$$\frac{\partial \rho(\bar{\nu}, t)}{\partial t} > 0 \tag{5}$$

(over an observable range of t) represents a minimum requirement for Eq. 3 to obtain.

The temporal behavior of $\rho(\bar{\nu}, t)$ for the TNS-apomyoglobin complex at 4°C is illustrated in Fig. 5 at several emission wavelengths.[3] According to Eq. 1, condition 5 can only be satisfied for this system at the longer emission wavelengths.

It is expedient to consider a specific model based on Eq. 1 to illustrate relations 3 and 4 more explicitly. We take $\rho(\bar{\nu}, t)$ at fixed t to be represented by a Gaussian spectral contour[4]

$$\rho(\bar{\nu}, t) = e^{-a(\bar{\nu} - \xi(t))^2} \tag{6}$$

of half bandwidth $\Gamma = \sqrt{2.773/a}$. Both $i(t)$ and $\xi(t)$ are described with single relaxation times τ_f and τ_R, respectively,[5]

$$i(t) = \alpha e^{-t/\tau_f} \tag{7}$$

$$\xi(t) = \xi_\infty + \Delta\xi e^{-t/\tau_R}, \tag{8}$$

where the energy gap (total spectral shift) $\Delta\xi = \xi_0 - \xi_\infty$ is defined as the difference between the initial (ξ_0) and fully relaxed (ξ_∞) spectral positions, and α is proportional to the radiative transition probability.

Combining Eqs. 4, 6, and 7, we have

$$2a(\bar{\nu} - \xi(t)) \frac{\partial \xi(t)}{\partial t} > \tau_f^{-1}. \tag{9}$$

The longer the duration of this condition, the more observable the rise in $f(\bar{\nu}, t)$. Together, Eqs. 8 and 9 illustrate the specific dependence of condition 3 on elementary bandwidth, emission wavenumber, energy gap, spectral relaxation rate, and relative electronic relaxation rate. For example, since $[\partial\xi(t)/\partial t] < 0$, $\bar{\nu}$ must be chosen to the low energy side of $\xi(t)$ ($\bar{\nu} < \xi(t)$) and this inequality must be satisfied over the time range where condition 3 is valid.

Several of these dependencies are illustrated in the computer-simulated decay curves $f(\bar{\nu}, t)$ of Fig. 6, based on Eqs. 1, 6, 7, and 8. In each graph $f(\bar{\nu}, t)$ is shown at two emission wavelengths, 450 nm ($\bar{\nu} \sim 22$ kK) and 540 nm ($\bar{\nu} \sim 18.5$ kK). The common parameters in this figure are $\xi_0 = 23$ kK, $\tau_f = 10$ ns and $\Gamma = 5$ kK. Fig. 6A and B show the effect of a change in the extent of the total shift $\Delta\xi$. In Fig. 6A $\Delta\xi$ =

[3] See DeToma et al. (1976) for another example.

[4] In discussing Eqs. 3 and 4, the normalization of $\rho(\bar{\nu}, t)$ is arbitrary. In Eq. 1 $\int_0^\infty \rho(\bar{\nu}, t) d\bar{\nu} = 1$, formally.

[5] For the TNS-apomyoglobin system both $i(t)$ and $\xi(t)$ are operationally described by a minimum of two relaxation times; however, the discussion presented here does not require this added complication.

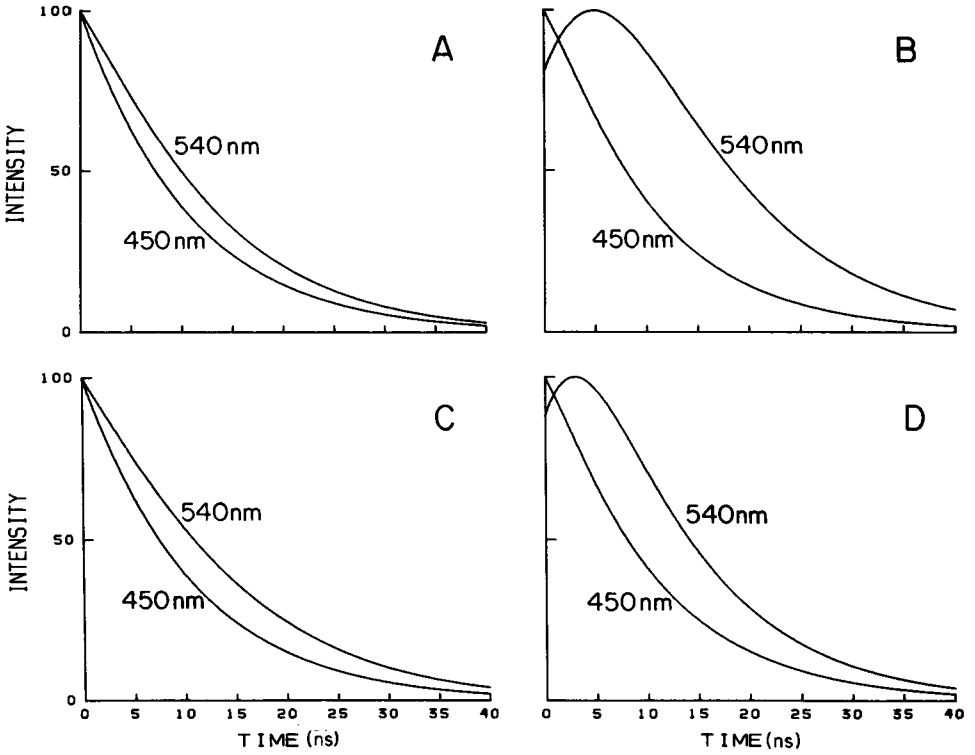

FIGURE 6 Simulated decay curves based on the Bakhshiev formulation of solvent relaxation. Graphs A and B illustrate a case where the energy gap ($\xi_0 - \xi_\infty$) has been increased by a factor of four, $B > A$. Graph A parameters: $\xi_\infty = 22.5$ kK, $\tau_R = 10$ ns; B parameters: $\xi_\infty = 21$ kK, $\tau_R = 10$ ns. Graphs C and D represent a case where the spectral relaxation rate parameter (τ_R^{-1}) has been increased by a factor of four, D > C. Graph C parameters: $\xi_\infty = 22$ kK, $\tau_R = 20$ ns, D parameters: $\xi_\infty = 22$ kK, $\tau_R = 5$ ns. Common parameters in each graph: $\xi_0 = 23$ kK, $\tau_f = 10$ ns, $\Gamma = 5$ kK, emission wavelengths 450 nm and 540 nm. See text for a more complete description of these parameters.

0.5 kK (close to what is observed with the TNS-apomyoglobin complex). In Fig. 6B τ_f and $\tau_R(\tau_f = \tau_R)$ remain unchanged but $\Delta\xi = 2$ kK (similar to that observed for TNS in glycerol) was increased by a factor of four. A clear rise in $f(\bar{\nu}, t)$ is apparent in B but only marginally present in A and only at the longer emission wavelength (540 nm). Fig. 6C and D illustrate the effect of a change in the rate of spectral relaxation, $\Delta\xi = 1$ kK being fixed in both graphs. A decrease in τ_R from 20 ns in Fig. 6C to 5 ns in 6D introduces a rise in the 540-nm decay that is not readily apparent in Fig. 6C.

It is important to distinguish the behavior described above from the limiting behavior.

$$\frac{\partial \rho}{\partial t} \to 0, \tag{10}$$

where the spectral system is stationary during the observation time window. Condition

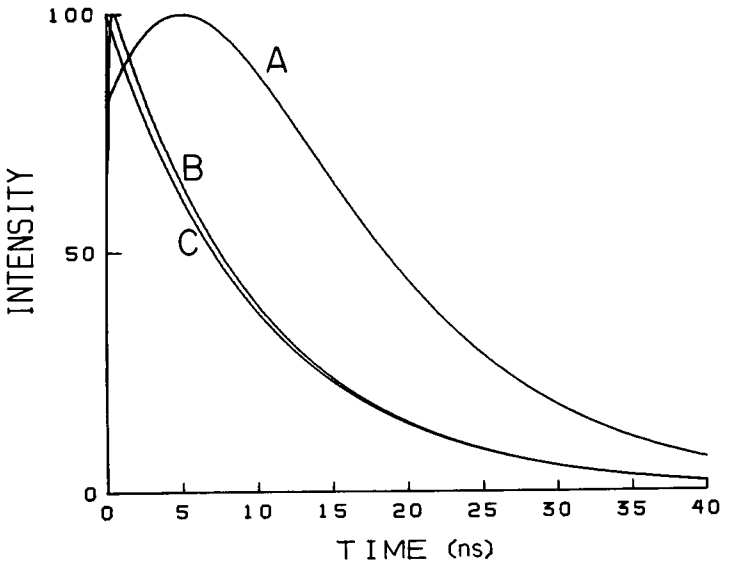

FIGURE 7 Simulated decay curves based on the Bakhshiev formulation of solvent relaxation. Curve A: $\tau_R = \tau_f$, curve B: $\tau_R = 0.01\ \tau_f$, curve C: $\tau_R = 100\ \tau_f$. Common parameters: $\tau_f = 10$ ns, $\xi_0 = 23$ kK, $\xi_\infty = 22$ kK, $\lambda_{em} = 540$ nm, $\Gamma = 5$ kK.

10 implies that $\xi(t) \approx \xi_0$ or $\xi(t) \approx \xi_\infty$, corresponding to the extreme relations between τ_f and τ_R, $\tau_f \ll \tau_R$ or $\tau_f \gg \tau_R$, respectively. Under this limiting behavior relation 3 will not be satisfied over a significant time period. Simulated decay curves based on Eqs. 1, 6, 7, and 8 that illustrate this point are shown in Fig. 7. These decay curves were generated at 540 nm (red tail of the steady-state emission spectrum) with the common parameters $\tau_f = 10$ ns, $\xi_0 = 23$ kK, $\xi_\infty = 22$ kK, and $\Gamma = 5$ kK. For curve A, $\tau_R = \tau_f$ and a rise of significant duration is clearly present. When $\tau_R = 0.01\ \tau_f$ (curve B) a brief rise in $f(\bar{\nu}, t)$ is just evident, while the rise is not apparent in curve C where $\tau_R = 100\ \tau_f$. The normalized decay curves B and C approach each other in this limit as is implied by relation 10.

Based on this discussion, the results shown in Table I for the 2,6 *p*-TNS apomyoglobin complex are consistent with the general model of Bakhshiev et al. (1966). It is reasonable to propose that a portion of the emission is due to species formed in the excited state in spite of the small contribution by terms with a negative amplitude. The rate of the time-dependent red shift, $\bar{\nu}_{max}(t)$, is faster at 20°C than at 4°C. Thus the more significant term with a negative amplitude found at 20° may be explained in terms of the changed relation between $\bar{\nu}_{max}(t)$ and $i(t)$ at the two temperatures.

It is concluded that the fluorescence decay kinetics of the 2,6 *p*-TNS-apomyoglobin complex depend on the emission wavelength. The most reasonable interpretation of the decay kinetics and the time-resolved emission spectra is that an excited-state reaction leads to emission from states of lower energy. The excited-state phenomena described here are qualitatively similar to those found when 2,6 *p*-TNS is dissolved in a

viscous solvent such as glycerol. It is suggested that they originate in interactions, on the nanosecond time scale, between the dye and its environment. Due to the hydrophobic nature of the binding site, these interactions may involve specific amino acid residues at the apoprotein binding site.

The *N*-arylaminonaphthalene sulfonate dyes have been used to obtain information regarding the polarity at biological binding sites (Brand and Gohlke, 1972). Interpreting the fluorescence data in this manner has been criticized by Kosower et al. (1975). There can be no doubt that in homogeneous fluid solutions (where $\tau_R \ll \tau_f$), the fluorescence emission maxima of these dyes are strongly influenced by solvent polarity and hence they may be used as "polarity probes." In viscous solvents, like glycerol, or in many biological binding sites, τ_R and τ_f are of comparable magnitude and thus emission takes place, to a large extent, from states that are not fully relaxed. As a result in these cases, the steady-state emission spectra are shifted to higher energy, than that observed for a fluid solvent of the same polarity. It is essential that environmental interactions in such systems be described in terms of kinetic parameters. Moreover, a biological binding site, unlike a homogeneous liquid, is anisotropic and the dye may undergo specific interactions with certain residues of the binding site. Thus, the characteristics of a biological binding site, studied by such dyes, are ill defined in terms of a single number such as the dielectric constant, which may be used to specify a liquid of low viscosity. The steady-state emission properties will be determined by all the above-mentioned parameters and a one-to-one correspondence with polarity cannot be expected. Time-resolved emission spectroscopy, on the other hand, provides a kinetic description of these environmental interactions from which additional information can be obtained about the character (to what extent the binding site resembles a homogeneous solvent with respect to the dye) and about the mobility of polar residues, including water, at biological sites of interest.

We are grateful to Prof. A. Nason for the use of a Cary spectrophotometer (Cary Instruments, Fairfield, N.J.). We thank Prof. E. Bucci for advice concerning the preparation of apomyoglobin, and Prof. W. Love for providing the method used for the determination of hemin concentrations.

This work was supported by National Institutes of Health Grant GM 11632. Dr. Gafni was supported by a U.S.A. State Department Grant, Dr. DeToma by NIH Postdoctural Fellowship 1 F32 GM01268, Dr. Manrow by NIH Training Grant GM5T01-G57, and Dr. Brand by NIH Career Development Award GM 10245.

This is publication 885 from the McCollum-Pratt Institute.

Received for publication 7 September 1976 and in revised form 22 October 1976.

REFERENCES

ANDERSON, S. R., M. BRUNORI, and G. WEBER. 1970. Fluorescence studies of aplysia and sperm whale apomyoglobins. *Biochemistry.* **9**:4723.

BAKHSHIEV, N. G., Y. T. MAZURENKO, and I. Y. PITERSKAYA. 1966. Luminescence decay in different portions of the luminescence spectrum of molecules in viscous solutions. *Opt. Spectrosc.* **21**:307.

BRAND, L., J. R. GOHLKE, and D. S. RAO. 1967. Evidence for binding of rose bengal and anilinonaphthalenesulfonates at the active site regions of liver alcohol dehydrogenase. *Biochemistry.* **6**:3510.

BRAND, L., and J. R. GOHLKE. 1972. Fluorescence probes for structure. *Annu. Rev. Biochem.* **41**:843.

DeToma, R. P., J. H. Easter, and L. Brand. 1976. Dynamic interactions of fluorescence probes with the solvent environment. *J. Am. Chem. Soc.* **98**:5001.

Easter, J. H., R. P. DeToma, and L. Brand. 1976. Nanosecond time-resolved emission spectroscopy of a fluorescence probe adsorbed to L-α-egg lecithin vesicles. *Biophys. J.* **16**:571.

Edelman, G. M., and W. O. McClure. 1968. Fluorescence probes and the conformation of proteins. *Accounts Chem. Res.* **1**:65.

Gafni, A., R. L. Modlin, and L. Brand. 1975. Analysis of fluorescence decay curves by means of the Laplace transformation. *Biophys. J.* **15**:263.

Greene, F. C. 1975. Neutral and cationic sulfonamido derivatives of the fluorescent probe 2-p-toluidinyl-naphthalene-6-sulfonate. Properties and mechanistic implications. *Biochemistry.* **14**:747.

Grinvald, A., and I. Z. Steinberg. 1974. On the analysis of fluorescence decay kinetics by the method of least squares. *Anal. Biochem.* **59**:583.

Kosower, E. M., H. Dodiuk, K. Tanizawa, M. Ottolenghi, and N. Orbach. 1975. Intramolecular donor-acceptor systems. Radiative and nonradiative processes for the excited states of 2-N-arylamino-6-sulfonates. *J. Am. Chem. Soc.* **97**:2167.

Li, Y. H., L. M. Chan, L. Tyer, R. T. Moody, C. M. Himel, and D. M. Hercules. 1975. Study of solvent effects on the fluorescence of 1-(dimethylamino)-5-naphthalenesulfonic acid and related compounds. *J. Am. Chem. Soc.* **97**:3118.

McClure, W. O., and G. M. Edelman. 1966. Fluorescence probes for comformational states of proteins. I. Mechanism of fluorescence of 2-p-toluidinylnaphthalene-6-sulfonate, a hydrophobic probe. *Biochemistry.* **5**:1908.

Penzer, G. R. 1972. 1-Anilinonaphthalene-8-sulphonate. The dependence of emission spectra on the molecular conformation studied by fluorescence and proton-magnetic resonance. *Eur. J. Biochem.* **25**:218.

Seliskar, C. J., and L. Brand. 1971. Electronic spectra of 2-aminonaphthalene-6-sulfonate and related molecules. I. General properties and excited-state reactions. *J. Am. Chem. Soc.* **93**:5405.

Shinitzky, M. 1972. Effect of fluorescence polarization on intensity and decay measurements. *J. Chem. Phys.* **56**:5979.

Smith, J. C., and R. W. Woody. 1976. Molecular orbital calculations of *N*-phenylnaphthylamines. Fluorescence and circular dichroism probes. *J. Phys. Chem.* **80**:1094.

Stryer, L. 1965. The interaction of a naphthalene dye with apomyoglobin and apohemoglobin. A fluorescent probe of non-polar binding sites. *J. Mol. Biol.* **13**:482.

Theorell, H., and Å. Åkeson. 1955. Reversible splitting of a homogeneous horse myoglobin. *Ann. Acad. Sci. Fenn. Ser. A, II Chem.* **60**:303.

Turner, D. C., and L. Brand. 1968. Quantitative estimation of protein binding site polarity. Fluorescence of N-arylaminonaphthalenesulfonates. *Biochemistry.* **7**:3381.

Weber, G., and D. J. R. Laurence. 1954. Fluorescence indicators of adsorption in aqueous solution and on the solid phase. *Biochem. J.* **56**:XXXI.